

# Coherent Turbo Coded MIMO OFDM

K. Vasudevan

Dept. of EE  
IIT Kanpur  
India

Email: vasu@iitk.ac.in

**Abstract**—The minimum average signal-to-noise ratio (SNR) per bit required for error-free transmission over a fading channel is derived, and is shown to be equal to that of the additive white Gaussian noise (AWGN) channel, which is  $-1.6$  dB. Discrete-time algorithms are presented for timing and carrier synchronization, as well as channel estimation, for multiple input multiple output (MIMO) orthogonal frequency division multiplexed (OFDM) systems. The algorithms can be implemented on programmable hardware and there is a large scope for parallel processing.

**Index Terms**—MIMO; OFDM; coherent detection; matched filtering; turbo codes; frequency selective Rayleigh fading; channel capacity.

## I. INTRODUCTION

As the world prepares for 5G [1]–[3] with its capabilities like gigabits per second peak data rate for each user, smart antennas, massive multiple input multiple output (MIMO) transmitters and receivers [4]–[6] and millimeter wave frequencies [7]–[10], the question remains [11]: What is the operating signal-to-noise ratio (SNR) per bit of the present day mobile phones? The mobile phones indicate a typical received signal strength of  $-100$  dBm ( $10^{-10}$  mW), however this is not the SNR per bit. It appears that the research in telecommunications engineering is primarily driven by two groups namely the RF (radio frequency) and microelectronics. It also appears that advancement of technology implies asking for more: more data rate, more bandwidth, more antennas and finally more transistors on a single chip. However, there is yet another group in telecommunications, which asks for less. This is the algorithms group (perhaps this group has been too busy writing too many complicated equations) for the physical layer of telecommunication systems. The task of this group is to develop discrete-time algorithms that would minimize the bite-error-rate, by consuming the minimum possible transmit power. This aspect of telecommunications is expected to assume significance in future.

The main contribution of this paper is to develop discrete-time algorithms for coherently detecting multiple input, multiple output (MIMO), orthogonal frequency division multiplexed (OFDM) signals, transmitted over frequency selective Rayleigh fading channels. Carrier frequency offset and additive white Gaussian noise (AWGN) are the other impairments considered in this work. The minimum SNR per bit required for error-free transmission over MIMO channels is derived. The capacity of single-user MIMO systems under different

assumptions about the channel impulse response (also called the channel state information or CSI) and the statistics of the channel impulse response (also called channel distribution information or CDI) is discussed in [12]. The capacity of MIMO Rayleigh fading channels in the presence of interference and receive correlation is discussed in [13]. The low SNR capacity of MIMO fading channels with imperfect channel state information is presented in [14]. To the best of our knowledge, other than the work in [15], which deals with turbo coded single input single output (SISO) OFDM, and [11] [16], which deal with turbo coded single input multiple output (SIMO) OFDM, discrete-time algorithms for the coherent detection of turbo coded MIMO OFDM systems have not been discussed earlier in the literature. Simulations results for a  $2 \times 2$  turbo coded MIMO OFDM system indicate that a BER of  $10^{-5}$ , is obtained at an SNR per bit of just 5.5 dB, which is a 2.5 dB improvement over the performance given in [11].

This paper is organized as follows. Section II presents the system model. The discrete-time algorithms for the coherent receiver are given in Section III. The simulation results are presented in Section IV. Finally, Section V concludes the paper.

## II. SYSTEM MODEL

We assume a MIMO-OFDM system with  $N_t$  transmit and  $N_r$  receive antennas, with QPSK modulation. The data from each transmit antenna is organized into frames, as shown in Fig. 1(a), similar to [11] [15] [16]. Note the presence of the cyclic suffix, whose purpose will be explained later. In Fig. 1(b), we observe that only the data and postamble QPSK symbols are interleaved. The buffer QPSK symbols ( $B$ ) are sent to the IFFT without interleaving. In Fig. 1, the subscript  $k$  refers to the  $k^{th}$  frame,  $n$  denotes the time index in a frame and  $1 \leq n_t \leq N_t$  is the index to the transmit antenna. The total length of the frame is

$$L = L_p + L_{cs} + L_{cp} + L_d. \quad (1)$$

Let us assume a channel span equal to  $L_h$ . The channel span assumed by the receiver is [15] [16]

$$L_{hr} = 2L_h - 1 \quad (2)$$

Note that  $L_h$  depends on the delay spread of the channel, and is measured in terms of the number of symbols. Recall that, the delay spread is a measure of the time difference between

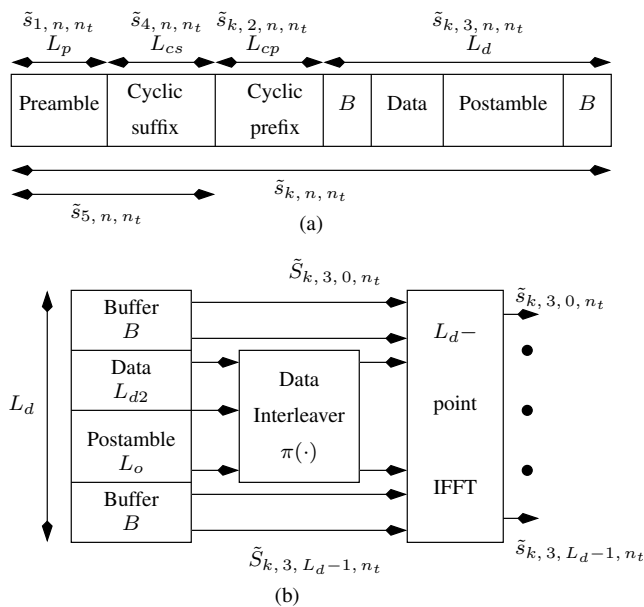


Fig. 1. The frame structure in the time domain.

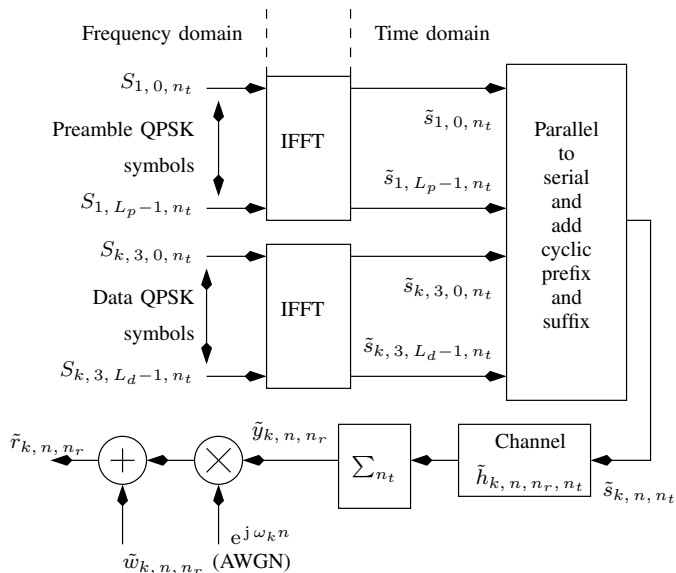


Fig. 2. Block diagram of the transmitter.

the arrival of the first and the last multipath signal, as seen by the receiver. Typically

$$L_h = d_0 / (cT_s) \quad (3)$$

where  $d_0$  is the distance between the longest and shortest multipath,  $c$  is the velocity of light and  $T_s$  is the symbol duration. We have assumed a situation where the mobile is close to the base station and the longest path is reflected from the cell edge, which is approximately equal to the cell diameter  $d_0$ , as shown in Fig. 3. For  $L_h = 10$ ,  $1/T_s = 10^7$  bauds and  $c = 3 \times 10^8$  meters per sec, we get  $d_0 = 300$  meters. Similarly with  $L_h = 10$  and  $1/T_s = 10^8$  bauds we obtain  $d_0 = 30$

meters. In other words, as the baud rate increases, the cell size needs to decrease, and consequently the transmit power decreases, for the same channel span  $L_h$ . The length of the cyclic prefix and suffix is [17]:

$$L_{cp} = L_{cs} = L_{hr} - 1. \quad (4)$$

Throughout the manuscript, we use tilde to denote complex quantities. However, complex QPSK symbols will be denoted without a tilde e.g.,  $S_{1,n,n_t}$ . Boldface letters denote vectors or matrices. The channel coefficients  $\tilde{h}_{k,n,n_r,n_t}$  associated with the receive antenna  $n_r$  ( $1 \leq n_r \leq N_r$ ) and transmit antenna  $n_t$  ( $1 \leq n_t \leq N_t$ ) for the  $k^{\text{th}}$  frame are  $\mathcal{CN}(0, 2\sigma_f^2)$  and independent over time  $n$ , that is:

$$\frac{1}{2} E \left[ \tilde{h}_{k,n,n_r,n_t} \tilde{h}_{k,n-m,n_r,n_t}^* \right] = \sigma_f^2 \delta_K(m) \quad (5)$$

where “\*” denotes complex conjugate and  $\delta_K(\cdot)$  is the Kronecker delta function. This implies a uniform power delay profile. Note that a uniform power delay profile is the worst case channel model, since all the multipath components have the same power. The channel is assumed to be quasi-static, that is  $\tilde{h}_{k,n,n_r,n_t}$  is time-invariant over one frame and varies independently from frame-to-frame. The AWGN noise samples  $\tilde{w}_{k,n,n_r}$  for the  $k^{\text{th}}$  frame at time  $n$  and receive antenna  $n_r$  are  $\mathcal{CN}(0, 2\sigma_w^2)$ . The frequency offset  $\omega_k$  for the  $k^{\text{th}}$  frame is uniformly distributed over  $[-0.04, 0.04]$  radian [18]. We assume that  $\omega_k$  is fixed for a frame and varies randomly from frame-to-frame. The block diagram of the transmitter is given in Fig. 2.

With reference to Fig. 1(a) and 2, note that:

$$\begin{aligned} \tilde{s}_{1,n,n_t} &= \frac{1}{L_p} \sum_{i=0}^{L_p-1} S_{1,i,n_t} e^{j2\pi ni/L_p} \\ &\quad \text{for } 0 \leq n \leq L_p - 1 \\ \tilde{s}_{k,3,n,n_t} &= \frac{1}{L_d} \sum_{i=0}^{L_d-1} S_{k,3,i,n_t} e^{j2\pi ni/L_d} \\ &\quad \text{for } 0 \leq n \leq L_d - 1 \\ \tilde{s}_{k,2,n,n_t} &= \tilde{s}_{k,3,L_d-L_{cp}+n,n_t} \\ &\quad \text{for } 0 \leq n \leq L_{cp} - 1 \\ \tilde{s}_{4,n,n_t} &= \tilde{s}_{1,n,n_t} \\ &\quad \text{for } 0 \leq n \leq L_{cs} - 1 \\ \tilde{s}_{5,n,n_t} &= \tilde{s}_{1,n,n_t} + \tilde{s}_{4,n-L_p,n_t}. \end{aligned} \quad (6)$$

From (6), it is clear that the preamble is independent of the frame  $k$ . However, each transmit antenna has its own preamble, for the purpose of synchronization and channel estimation at the receiver.

The preamble in the frequency domain, for each transmit antenna is generated as follows. Let  $\pi_p(i)$ , for  $0 \leq i \leq L_p - 1$ , denote the interleaver map for the preamble. Let

$$\mathbf{S}_r = \left[ S_{r,0} \quad \dots \quad S_{r,L_p-1} \right]_{L_p \times 1}^T \quad (7)$$

denote a random vector of QPSK symbols. The preamble vector for the transmit antenna  $n_t$  is first initialized by

$$\begin{aligned} \mathbf{S}_{1, n_t} &= [S_{1, 0, n_t} \cdots S_{1, L_p - 1, n_t}]_{L_p \times 1}^T \\ &= \mathbf{0}_{L_p \times 1}. \end{aligned} \quad (8)$$

Next, we substitute

$$\mathbf{S}_{1, \pi_p(i_4:i_5), n_t} = \mathbf{S}_r(i_4 : i_5). \quad (9)$$

where  $i_4 : i_5$  denotes the range of indices from  $i_4$  to  $i_5$ , both inclusive, and

$$\begin{aligned} i_4 &= (n_t - 1)L_p/N_t \\ i_5 &= i_4 + L_p/N_t - 1. \end{aligned} \quad (10)$$

Note that the preamble in the frequency domain for each transmit antenna has only  $L_p/N_t$  non-zero elements, the rest of the elements are zero. Moreover, due to  $\pi_p(\cdot)$ , the  $L_p/N_t$  non-zero elements are randomly interspersed over the  $L_p$  subcarriers in the frequency domain, for each transmit antenna.

By virtue of the preamble construction in (8), (9) and (10), the preambles in the frequency and time domains corresponding to transmit antennas  $n_t$  and  $m_t$  satisfy the relation (using Parseval's energy theorem):

$$\begin{aligned} S_{1, i, n_t} S_{1, i, m_t}^* &= (2N_t L_p / L_d) \delta_K(n_t - m_t) \\ &\quad \text{for } 0 \leq i \leq L_p - 1 \\ \Rightarrow \tilde{s}_{1, n, n_t} \odot_{L_p} \tilde{s}_{1, -n, m_t}^* &= \begin{cases} 0 & \text{for } n_t \neq m_t, \\ (2L_p / L_d) \delta_K(n) & \text{for } n_t = m_t \end{cases} \end{aligned} \quad (11)$$

where " $\odot_{L_p}$ " denotes the  $L_p$ -point circular convolution. In other words, the preambles corresponding to distinct transmit antennas are orthogonal over  $L_p$  samples. Moreover, the autocorrelation of the preambles in frequency and time domain, can be approximated by a weighted Kronecker delta function (this condition is usually satisfied by random sequences having zero-mean; the approximation gets better as  $L_p$  increases).

We assume  $S_{k, 3, i, n_t} \in \{\pm 1 \pm j\}$ . Since we require:

$$E[|\tilde{s}_{1, n, n_t}|^2] = E[|\tilde{s}_{k, 3, n, n_t}|^2] = 2/L_d \triangleq \sigma_s^2 \quad (12)$$

we must have  $S_{1, i, n_t} \in \sqrt{L_p N_t / L_d} (\pm 1 \pm j)$ . In other words, the average power of the preamble part must be equal to the average power of the data part, in the time domain.

Due to the presence of the cyclic suffix in Fig. 1 and (6), and due to (11), we have

$$\begin{aligned} \tilde{s}_{5, n, n_t} \star \tilde{s}_{1, L_p - 1 - n, m_t}^* &= \begin{cases} 0 & \text{for } L_p - 1 \leq n \leq L_p + L_{hr} - 2, \\ & n_t \neq m_t \\ (2L_p / L_d) \delta_K(n - L_p + 1) & \text{for } n_t = m_t \end{cases} \end{aligned} \quad (13)$$

where " $\star$ " denotes linear convolution.

The signal for the  $k^{th}$  frame and receive antenna  $n_r$  can be written as (for  $0 \leq n \leq L + L_h - 2$ ):

$$\begin{aligned} \tilde{r}_{k, n, n_r} &= \sum_{n_t=1}^{N_t} \left( \tilde{s}_{k, n, n_t} \star \tilde{h}_{k, n, n_r, n_t} \right) e^{j\omega_k n} + \tilde{w}_{k, n, n_r} \\ &= \tilde{y}_{k, n, n_r} e^{j\omega_k n} + \tilde{w}_{k, n, n_r} \end{aligned} \quad (14)$$

where  $\tilde{s}_{k, n, n_t}$  is depicted in Fig. 1(a) and

$$\tilde{y}_{k, n, n_r} = \sum_{n_t=1}^{N_t} \tilde{s}_{k, n, n_t} \star \tilde{h}_{k, n, n_r, n_t}. \quad (15)$$

Note that any random carrier phase can be absorbed in the channel impulse response.

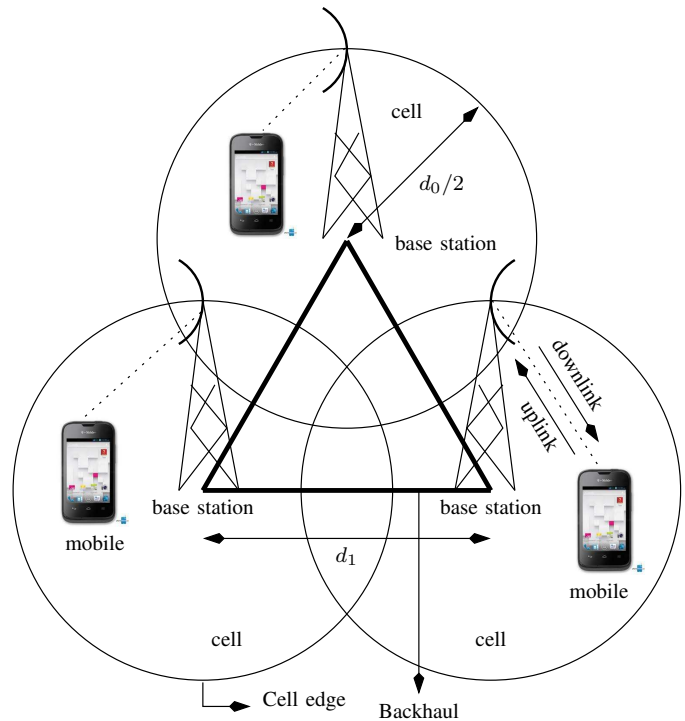


Fig. 3. System block diagram.

The system block diagram is depicted in Fig. 3. The base stations are interconnected by a high data-rate backhaul. Note that  $d_1 < d_0$ . In order to obtain symmetry, the backhaul forms an equilateral triangle of length  $d_1$ . The base station is at the center of each cell, whose diameter is  $d_0$ . The uplink and downlink transmissions between the mobiles and base station could be carried out using time division duplex (TDD) or frequency division duplex (FDD). Time division (TDMA), frequency division (FDMA), code division (CDMA), orthogonal frequency division (OFDMA), for downlink transmissions and filterbank multicarrier (FBMC), for uplink transmissions [19], are the possible choices for multiple access (MA) techniques.

### III. RECEIVER

In this section, we discuss the discrete-time receiver algorithms.

### A. Start of Frame (SoF) and Coarse Frequency Offset Estimate

The start of frame (SoF) detection and coarse frequency offset estimation is performed for each receive antenna  $1 \leq n_r \leq N_r$  and transmit antenna  $1 \leq n_t \leq N_t$ , as given by the following rule (similar to (22) in [15] and (24) in [16]): choose that value of  $m$  and  $\nu_k$  which maximizes

$$\left| (\tilde{r}_{k,m,n_r} e^{-j\nu_k m}) \star \tilde{s}_{1,L_p-1-m,n_t}^* \right|. \quad (16)$$

Let  $\hat{m}_k(\cdot)$  denote the time instant and  $\hat{\nu}_k(\cdot)$  denote the coarse estimate of the frequency offset (both of which are functions of  $n_r$  and  $n_t$ ), at which the maximum in (16) is obtained. Note that (16) is a two-dimensional search over  $m$  and  $\nu_k$ , which can be efficiently implemented in hardware, and there is a large scope for parallel processing. In particular, the search over  $\nu_k$  involves dividing the range of  $\omega_k$  ( $[-0.04, 0.04]$  radians) into  $B_1$  frequency bins, and deciding in favour of that bin which maximizes (16). In our simulations,  $B_1 = 64$  [15] [16].

Note that in the absence of noise and due to the properties given in (13)

$$\hat{m}_k(n_r, n_t) = L_p - 1 + \operatorname{argmax}_m \left| \tilde{h}_{k,m,n_r,n_t} \right| \quad (17)$$

where  $\operatorname{argmax}_m$  corresponds to the value of  $m$  for which  $\left| \tilde{h}_{k,m,n_r,n_t} \right|$  is maximum. We also have

$$L_p - 1 \leq \hat{m}_k(n_r, n_t) \leq L_p + L_h - 2. \quad (18)$$

If  $\hat{m}_k(\cdot)$  lies outside the range in (18), the frame is declared as erased (not detected). This implies that the peak in (16) is due to noise, and not due to the channel. The average value of the coarse frequency offset estimate is given by

$$\hat{\omega}_k = \frac{\sum_{n_r=1}^{N_r} \sum_{n_t=1}^{N_t} \hat{\nu}_k(n_r, n_t)}{N_r N_t}. \quad (19)$$

### B. Channel Estimation

We assume that the SoF has been estimated using (16) with outcome  $m_{0,k}$  given by (assuming the condition in (18) is satisfied for all  $n_r$  and  $n_t$ ):

$$m_{0,k} = \hat{m}_k(1, 1) - L_p + 1 \quad 0 \leq m_{0,k} \leq L_h - 1 \quad (20)$$

and the frequency offset has been perfectly canceled [15] [16]. Observe that any value of  $n_r$  and  $n_t$  can be used in the computation of (20). We have taken  $n_r = n_t = 1$ . Define

$$m_{1,k} = m_{0,k} + L_h - 1. \quad (21)$$

For the sake of notational simplicity, we drop the subscript  $k$  in  $m_{1,k}$ , and refer to it as  $m_1$ . The steady-state, preamble part of the received signal for the  $k^{\text{th}}$  frame and receive antenna  $n_r$  can be written as:

$$\tilde{\mathbf{r}}_{k,m_1,n_r} = \sum_{n_t=1}^{N_t} \tilde{\mathbf{s}}_{5,n_t} \tilde{\mathbf{h}}_{k,n_r,n_t} + \tilde{\mathbf{w}}_{k,m_1,n_r} \quad (22)$$

where

$$\begin{aligned} \tilde{\mathbf{r}}_{k,m_1,n_r} &= \begin{bmatrix} \tilde{r}_{k,m_1,n_r} & \cdots & \tilde{r}_{k,m_1+L_p-1,n_r} \end{bmatrix}^T \\ &\quad [L_p \times 1] \text{ vector} \\ \tilde{\mathbf{w}}_{k,m_1,n_r} &= \begin{bmatrix} \tilde{w}_{k,m_1,n_r} & \cdots & \tilde{w}_{k,m_1+L_p-1,n_r} \end{bmatrix}^T \\ &\quad [L_p \times 1] \text{ vector} \\ \tilde{\mathbf{h}}_{k,n_r,n_t} &= \begin{bmatrix} \tilde{h}_{k,0,n_r,n_t} & \cdots & \tilde{h}_{k,L_{hr}-1,n_r,n_t} \end{bmatrix}^T \\ &\quad [L_{hr} \times 1] \text{ vector} \\ \tilde{\mathbf{s}}_{5,n_t} &= \begin{bmatrix} \tilde{s}_{5,L_{hr}-1,n_t} & \cdots & \tilde{s}_{5,0,n_t} \\ \vdots & \cdots & \vdots \\ \tilde{s}_{5,L_p+L_{hr}-2,n_t} & \cdots & \tilde{s}_{5,L_p-1,n_t} \end{bmatrix} \\ &\quad [L_p \times L_{hr}] \text{ matrix} \end{aligned} \quad (23)$$

where  $L_{hr}$  is the channel length assumed by the receiver (see (2)),  $\tilde{\mathbf{s}}_{5,n_t}$  is the channel estimation matrix and  $\tilde{\mathbf{r}}_{k,m_1,n_r}$  is the received signal vector *after* cancellation of the frequency offset. Observe that  $\tilde{\mathbf{s}}_{5,n_t}$  is independent of  $m_1$  and due to the relations in (11) and (13), we have

$$\tilde{\mathbf{s}}_{5,m_t}^H \tilde{\mathbf{s}}_{5,n_t} = \begin{cases} \mathbf{0}_{L_{hr} \times L_{hr}} & \text{for } n_t \neq m_t \\ (2L_p/L_d)\mathbf{I}_{L_{hr}} & \text{for } n_t = m_t \end{cases} \quad (24)$$

where  $\mathbf{I}_{L_{hr}}$  is an  $L_{hr} \times L_{hr}$  identity matrix and  $\mathbf{0}_{L_{hr} \times L_{hr}}$  is an  $L_{hr} \times L_{hr}$  null matrix. The statement of the ML channel estimation is as follows. Find  $\hat{\mathbf{h}}_{k,n_r,m_t}$  (the estimate of  $\tilde{\mathbf{h}}_{k,n_r,m_t}$ ) such that:

$$\begin{aligned} &\left( \tilde{\mathbf{r}}_{k,m_1,n_r} - \sum_{m_t=1}^{N_t} \tilde{\mathbf{s}}_{5,m_t} \hat{\mathbf{h}}_{k,n_r,m_t} \right)^H \\ &\left( \tilde{\mathbf{r}}_{k,m_1,n_r} - \sum_{m_t=1}^{N_t} \tilde{\mathbf{s}}_{5,m_t} \hat{\mathbf{h}}_{k,n_r,m_t} \right) \end{aligned} \quad (25)$$

is minimized. Differentiating with respect to  $\hat{\mathbf{h}}_{k,n_r,m_t}^*$  and setting the result to zero yields [17] [20]:

$$\hat{\mathbf{h}}_{k,n_r,m_t} = (\tilde{\mathbf{s}}_{5,m_t}^H \tilde{\mathbf{s}}_{5,m_t})^{-1} \tilde{\mathbf{s}}_{5,m_t}^H \tilde{\mathbf{r}}_{k,m_1,n_r}. \quad (26)$$

Observe that when  $m_{0,k} = L_h - 1$  in (20), and noise is absent (see (29) in [15] and (35) in [16]), we obtain:

$$\begin{aligned} &\hat{\mathbf{h}}_{k,n_r,m_t} \\ &= \begin{bmatrix} \tilde{h}_{k,0,n_r,m_t} & \cdots & \tilde{h}_{k,L_h-1,n_r,m_t} & 0 & \cdots & 0 \end{bmatrix}^T. \end{aligned} \quad (27)$$

Similarly, when  $m_{0,k} = 0$  and in the absence of noise:

$$\begin{aligned} &\hat{\mathbf{h}}_{k,n_r,m_t} \\ &= \begin{bmatrix} 0 & \cdots & 0 & \tilde{h}_{k,0,n_r,m_t} & \cdots & \tilde{h}_{k,L_h-1,n_r,m_t} \end{bmatrix}^T. \end{aligned} \quad (28)$$

To see the effect of noise on the channel estimate in (26), consider

$$\tilde{\mathbf{u}} = (\tilde{\mathbf{s}}_{5,m_t}^H \tilde{\mathbf{s}}_{5,m_t})^{-1} \tilde{\mathbf{s}}_{5,m_t}^H \tilde{\mathbf{w}}_{k,m_1,n_r}. \quad (29)$$

It can be shown that

$$E[\tilde{\mathbf{u}}\tilde{\mathbf{u}}^H] = \frac{\sigma_w^2 L_d}{L_p} \mathbf{I}_{L_{hr}} \triangleq 2\sigma_u^2 \mathbf{I}_{L_{hr}}. \quad (30)$$

Therefore, the variance of the ML channel estimate ( $\sigma_u^2$ ) tends to zero as  $L_p \rightarrow \infty$  and  $L_d$  is kept fixed. Conversely, when  $L_d$  is increased keeping  $L_p$  fixed, there is noise enhancement [11] [16].

### C. Fine Frequency Offset Estimation

The fine frequency offset estimate is obtained using the following rule: choose that value of time instant  $m$  and frequency offset  $\nu_{k,f}$  which maximizes:

$$\left| \left( \tilde{r}_{k,m,n_r} e^{-j(\hat{\omega}_k + \nu_{k,f})m} \right) \star \tilde{y}_{1,k,L_2-1-m,n_r,n_t}^* \right| \quad (31)$$

where

$$\begin{aligned} L_2 &= L_{hr} + L_p - 1 \\ \hat{y}_{1,k,m,n_r,n_t} &= \tilde{s}_{1,m,n_t} \star \hat{h}_{k,m,n_r,n_t} \end{aligned} \quad (32)$$

where  $\hat{h}_{k,m,n_r,n_t}$  is obtained from (26). The fine frequency offset estimate ( $\hat{\nu}_{k,f}(n_r, n_t)$ ) is obtained by dividing the interval  $[\hat{\omega}_k - 0.005, \hat{\omega}_k + 0.005]$  radian ( $\hat{\omega}_k$  is given in (19)) into  $B_2 = 64$  frequency bins [21]. The reason for choosing 0.005 radian can be traced to Fig. 5 of [16]. We find that the maximum error in the coarse estimate of the frequency offset is approximately 0.004 radian over  $10^4$  frames. Thus the probability that the maximum error exceeds 0.005 radian is less than  $10^{-4}$ . However, from Table V in this paper, we note that the maximum error in the frequency offset is  $2.4 \times 10^{-2}$  radians for  $L_p = 512$ , and  $1.1 \times 10^{-2}$  for  $L_p = 1024$ , both of which are larger than 0.005 radian. By observing this trend, we expect that for larger values of  $L_p$ , say  $L_p = 4096$ , the maximum error in the coarse frequency offset estimate would be less than 0.005 radians. Increasing  $L_p$  would also imply an increase in  $L_d$ , for the same throughput (see (51)). The average value of the fine frequency offset estimate is given by:

$$\hat{\omega}_{k,f} = \frac{\sum_{n_r=1}^{N_r} \sum_{n_t=1}^{N_t} \hat{\nu}_{k,f}(n_r, n_t)}{N_r N_t}. \quad (33)$$

### D. Super Fine Frequency Offset Estimation

The fine frequency offset estimate in (33) is still inadequate for turbo decoding and data detection when  $L_d \gg L_p$  [15]. Note that the residual frequency offset is equal to:

$$\omega_k - \hat{\omega}_k - \hat{\omega}_{k,f}. \quad (34)$$

This residual frequency offset is estimated by interpolating the FFT output and performing postamble matched filtering at the receiver [11] [16]. If the interpolation factor is  $I$ , then the FFT size is  $IL_d$  (interpolation in the frequency domain is achieved by zero-padding the FFT input in the time domain, and then taking the  $IL_d$ -point FFT). Let

$$m_{2,k} = m_{1,k} + L_p + L_{cs} \quad (35)$$

where  $m_{1,k}$  is defined in (21). Once again, we drop the subscript  $k$  from  $m_{2,k}$  and refer to it as  $m_2$ . Define the FFT input in the time domain as:

$$\tilde{\mathbf{r}}_{k,m_2,n_r} = [\tilde{r}_{k,m_2,n_r} \quad \cdots \quad \tilde{r}_{k,m_2+L_d-1,n_r}]^T \quad (36)$$

which is the data part of the received signal in (14) for the  $k^{\text{th}}$  frame and receive antenna  $n_r$ , assumed to have the residual frequency offset given by (34). The output of the  $IL_d$ -point FFT of  $\tilde{\mathbf{r}}_{k,m_2,n_r}$  in (36) is denoted by

$$\tilde{R}_{k,i,n_r} = \sum_{n=0}^{L_d-1} \tilde{r}_{k,m_2+n,n_r} e^{-j2\pi in/(IL_d)} \quad (37)$$

for  $0 \leq i \leq IL_d - 1$ .

The coefficients of the postamble matched filter is obtained as follows [11] [16]. Define

$$\tilde{G}_{k,i,n_r}'' = \sum_{n_t=1}^{N_t} \hat{H}_{k,i_3,n_r,n_t} S_{k,3,i,n_t} \quad \text{for } i_0 \leq i \leq i_1 \quad (38)$$

where  $\hat{H}_{k,i_3,n_r,n_t}$  is the  $L_d$ -point FFT of the channel estimate in (26), and

$$\begin{aligned} i_0 &= B + L_{d2} \\ i_1 &= i_0 + L_o - 1 \\ i_3 &= B + \pi(i - B) \end{aligned} \quad (39)$$

where  $\pi(\cdot)$  is the data interleaver map,  $B$ ,  $L_{d2}$  and  $L_o$  are the lengths of the buffer, data and postamble respectively, as shown in Fig. 1(b). Let

$$\tilde{G}_{k,i_3,n_r}' = \begin{cases} \tilde{G}_{k,i,n_r}'' & \text{for } i_0 \leq i \leq i_1 \\ 0 & \text{otherwise} \end{cases} \quad (40)$$

where  $0 \leq i_3 \leq L_d - 1$ , the relation between  $i_3$  and  $i$  is given in (39). Next, we perform interpolation:

$$\tilde{G}_{k,i_4,n_r} = \begin{cases} \tilde{G}_{k,i,n_r}' & \text{for } 0 \leq i \leq L_d - 1 \\ 0 & \text{otherwise} \end{cases} \quad (41)$$

where  $0 \leq i_4 \leq IL_d - 1$  and  $i_4 = iI$ . Finally, the postamble matched filter is  $\tilde{G}_{k,IL_d-1-i,n_r}^*$ , which is convolved with  $\tilde{R}_{k,i,n_r}$  in (37). Note that due to the presence of the cyclic prefix, any residual frequency offset in the time domain, manifests as a circular shift in the frequency domain. The purpose of the postamble matched filter is to capture this shift. The role of the buffer symbols is explained in [11] [16]. Assume that the peak of the postamble matched filter output occurs at  $m_{3,k}(n_r)$ . Ideally, in the absence of noise and frequency offset

$$m_{3,k}(n_r) = IL_d - 1. \quad (42)$$

In the presence of the frequency offset, the peak occurs to the left or right of  $IL_d - 1$ . The average superfine estimate of the residual frequency offset is given by:

$$\hat{\omega}_{k,sf} = 2\pi/(IL_d N_r) \sum_{n_r=1}^{N_r} [m_{3,k}(n_r) - IL_d + 1]. \quad (43)$$

### E. Noise Variance Estimation

The noise variance is estimated as follows, for the purpose of turbo decoding:

$$\hat{\sigma}_w^2 = \frac{1}{2L_p N_r} \sum_{n_r=1}^{N_r} \left( \tilde{\mathbf{r}}_{k, m_1, n_r} - \sum_{n_t=1}^{N_t} \tilde{\mathbf{s}}_{5, n_t} \hat{\mathbf{h}}_{k, n_r, n_t} \right)^H \left( \tilde{\mathbf{r}}_{k, m_1, n_r} - \sum_{n_t=1}^{N_t} \tilde{\mathbf{s}}_{5, n_t} \hat{\mathbf{h}}_{k, n_r, n_t} \right). \quad (44)$$

### F. Turbo Decoding

In this section, we assume that the frequency offset has been perfectly canceled, that is,  $\tilde{\mathbf{r}}_{k, m_2, n_r}$  in (36) contains no frequency offset. The output of the  $L_d$ -point FFT of  $\tilde{\mathbf{r}}_{k, m_2, n_r}$  for the  $k^{\text{th}}$  frame is given by:

$$\tilde{R}_{k, i, n_r} = \sum_{n_t=1}^{N_t} \tilde{H}_{k, i, n_r, n_t} S_{k, 3, i, n_t} + \tilde{W}_{k, i, n_r} \quad (45)$$

for  $0 \leq i \leq L_d - 1$ , where  $\tilde{H}_{k, i, n_r, n_t}$  is the  $L_d$ -point FFT of  $\tilde{h}_{k, n, n_r, n_t}$  and  $\tilde{W}_{k, i, n_r}$  is the  $L_d$ -point FFT of  $\tilde{w}_{k, n, n_r}$ . It can be shown that [15] [16]

$$\begin{aligned} \frac{1}{2} E \left[ \left| \tilde{W}_{k, i, n_r} \right|^2 \right] &= L_d \sigma_w^2 \\ \frac{1}{2} E \left[ \left| \tilde{H}_{k, i, n_r, n_t} \right|^2 \right] &= L_h \sigma_f^2. \end{aligned} \quad (46)$$

The generating matrix of each of the constituent encoders is given by (41) in [16]. For the purpose of turbo decoding, we consider the case where  $N_r = N_t = 2$ . The details of turbo decoding can be found in [16], and will not be discussed here. Suffices to say that corresponding to the transition from state  $m$  to state  $n$ , at decoder 1, for the  $k^{\text{th}}$  frame, at time  $i$ , we define (for  $0 \leq i \leq L_{d2} - 1$ ):

$$\gamma_{1, k, i, m, n} = \exp \left( -Z_{1, k, i, m, n} / (2L_d \hat{\sigma}_w^2) \right) \quad (47)$$

where  $Z_{1, k, i, m, n}$  is given by

$$\min_{\text{all } S_{m, n, 2}} \sum_{n_r=1}^2 \left| \tilde{R}_{k, i, n_r} - \sum_{n_t=1}^2 \hat{H}_{k, i, n_r, n_t} S_{m, n, n_t} \right|^2 \quad (48)$$

where  $S_{m, n, n_t}$  denotes the QPSK symbol corresponding to the transition from state  $m$  to state  $n$  in the trellis, at transmit antenna  $n_t$ . Observe that  $\hat{\sigma}_w^2$  is the estimate of  $\sigma_w^2$  obtained from (44). Observe that the minimization in (48) is over all possible QPSK symbols, at  $n_t = 2$  and index  $i$ . Similarly, for the transition from state  $m$  to state  $n$ , at decoder 2, for the  $k^{\text{th}}$  frame, at time  $i$ , we define (for  $0 \leq i \leq L_{d2} - 1$ ):

$$\gamma_{2, k, i, m, n} = \exp \left( -Z_{2, k, i, m, n} / (2L_d \hat{\sigma}_w^2) \right) \quad (49)$$

where  $Z_{2, k, i, m, n}$  is given by

$$\min_{\text{all } S_{m, n, 1}} \sum_{n_r=1}^2 \left| \tilde{R}_{k, i, n_r} - \sum_{n_t=1}^2 \hat{H}_{k, i, n_r, n_t} S_{m, n, n_t} \right|^2. \quad (50)$$

Now, (47) and (49) are used in the forward and backward recursions of the BCJR algorithm [16].

### G. Summary of the Receiver Algorithms

The receiver algorithms are summarized as follows:

- 1) Estimate the start-of-frame and the frequency offset (coarse) using (16), for each receive antenna. Obtain the average value of the frequency offset ( $\hat{\omega}_k$ ) using (19).
- 2) Cancel the frequency offset by multiplying  $\tilde{r}_{k, n, n_r}$  in (14) by  $e^{-j\hat{\omega}_k n}$ , and estimate the channel using (26), for each  $n_r$  and  $n_t$ .
- 3) Obtain  $\tilde{y}_{1, k, m, n_r, n_t}$  from (32) and the fine frequency offset using (33).
- 4) Cancel the frequency offset by multiplying  $\tilde{r}_{k, n, n_r}$  in (14) by  $e^{-j(\hat{\omega}_k + \hat{\omega}_{k, f})n}$ , and estimate the channel again using (26), for each  $n_r$  and  $n_t$ .
- 5) Obtain the average superfine frequency offset estimate using (43). Cancel the offset by multiplying  $\tilde{r}_{k, n, n_r}$  in (14) by  $e^{-j(\hat{\omega}_k + \hat{\omega}_{k, f} + \hat{\omega}_{k, sf})n}$ .
- 6) Obtain the noise variance estimate from (44).
- 7) Take the  $L_d$ -point FFT of  $\tilde{r}_{k, m_2, n_r}$  and perform turbo decoding.

## IV. SIMULATION RESULTS

In this section, we present the simulation results for the proposed turbo coded MIMO OFDM system with  $N_t = N_r = 2$ . The SNR per bit is defined in (61). Note that one data bit (two coded QPSK symbols) is sent simultaneously from two transmit antennas. Hence, the number of data bits sent from each transmit antenna is  $\kappa = 0.5$ , as given in (61). We have also assumed that  $\sigma_f^2 = 0.5$ . The frame parameters are summarized in Table I. The throughput is defined as [11] [16]:

TABLE I  
FRAME PARAMETERS.

Parameter	Value (QPSK symbols)
$L_p$	512, 1024
$L_d$	4096
$B$	4
$L_o$	256, 512
$L_{d2}$	3832, 3576
$L_h$	10
$L_{cp} = L_{cs}$	18

$$\mathcal{T} = \frac{L_{d2}}{L_d + L_p + L_{cp} + L_{cs}}. \quad (51)$$

The throughput of various frame configurations is given in Table II. The BER simulation results for the turbo coded MIMO OFDM system with  $N_t = N_r = 2$  is shown in Fig. 4. Here ‘‘Id’’ denotes the ideal receiver. For the practical receivers (‘‘Pr’’), the interpolation factor for superfine frequency offset estimation is  $I = 16$ . The practical receiver with  $L_p = 1024$ ,  $L_o = 512$  attains a BER of  $10^{-5}$  at an SNR per bit of 5.5 dB, which is 1 dB better than the receiver

TABLE II  
THROUGHPUT.

$L_p$	$L_o$	$L_{d2}$	$\mathcal{T}$
512	256	3832	82.515%
1024	512	3576	69.356%

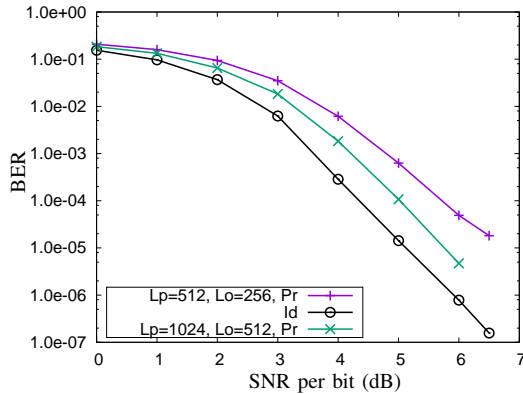


Fig. 4. BER simulation results.

with  $L_p = 512$ ,  $L_o = 256$ . This is due to the fact that the variance of the channel estimation error with  $L_p = 512$  is twice that of  $L_p = 1024$  (see (30)). This difference in the variance of the channel estimation error affects the turbo decoding process. Moreover, the practical receiver in Fig. 4 with  $L_p = 1024$ ,  $L_o = 512$  is 2.5 dB better than the practical receiver with one transmit and two receive antennas in Fig. 10 of [11]. The probability of frame erasure (this happens when

 TABLE III  
PROBABILITY OF FRAME ERASURE.

Frame configuration	Probability of erasure
$L_p = 512$ , $L_o = 256$	$2.98 \times 10^{-2}$
$L_p = 1024$ , $L_o = 512$	$7 \times 10^{-4}$

(18) is not satisfied) at 0 dB SNR per bit is shown in Table III. Clearly, as  $L_p$  increases, the probability of erasure decreases.

 TABLE IV  
RMS FREQUENCY OFFSET ESTIMATION ERROR.

Frame configuration	Coarse	Fine	Superfine
$L_p = 512$ $L_o = 256$	$1.71 \times 10^{-3}$	$3.38 \times 10^{-4}$	$5.85 \times 10^{-5}$
$L_p = 1024$ $L_o = 512$	$3.3 \times 10^{-4}$	$9.2 \times 10^{-5}$	$4.3 \times 10^{-5}$

Finally, the root mean square (RMS) and maximum frequency

 TABLE V  
MAXIMUM FREQUENCY OFFSET ESTIMATION ERROR.

Frame configuration	Coarse	Fine	Superfine
$L_p = 512$ $L_o = 256$	$2.4 \times 10^{-2}$	$1.6 \times 10^{-2}$	$2.6 \times 10^{-4}$
$L_p = 1024$ $L_o = 512$	$1.2 \times 10^{-2}$	$3.9 \times 10^{-4}$	$1.82 \times 10^{-4}$

offset estimation errors in radians, at 0 dB SNR per bit, are given in Tables IV and V.

## V. CONCLUSIONS

Discrete-time algorithms for the coherent detection of turbo coded MIMO OFDM system are presented. Simulations results for a  $2 \times 2$  turbo coded MIMO OFDM system indicate that a BER of  $10^{-5}$ , is obtained at an SNR per bit of just 5.5 dB, which is a 2.5 dB improvement over the performance given in the literature. The minimum average SNR per bit for error-free transmission over fading channels is derived and shown to be equal to  $-1.6$  dB, which is the same as that for the AWGN channel.

Future work could address the issues of peak-to-average power ratio (PAPR) and extension of the proposed concepts to massive MIMO systems.

## APPENDIX

### A. The Minimum Average SNR per bit for Error-free Transmission over Fading Channels

In this appendix, we derive the minimum average SNR per bit for error-free transmission over MIMO fading channels. Consider the signal

$$\tilde{r}_n = \tilde{x}_n + \tilde{w}_n \quad \text{for } 0 \leq n < N \quad (52)$$

where  $\tilde{x}_n$  is the transmitted signal (message) and  $\tilde{w}_n$  denotes samples of zero-mean noise, not necessarily Gaussian. All the terms in (52) are complex-valued or two-dimensional and are transmitted over one complex dimension. Here the term dimension refers to a communication link between the transmitter and the receiver carrying only real-valued signals. We also assume that  $\tilde{x}_n$  and  $\tilde{w}_n$  are ergodic random processes, that is, the time average statistics is equal to the ensemble average. The time-averaged signal power over two-dimensions is given by, for large values of  $N$ :

$$\frac{1}{N} \sum_{n=0}^{N-1} |\tilde{x}_n|^2 = P'_{av}. \quad (53)$$

The time-averaged noise power per dimension is

$$\frac{1}{2N} \sum_{n=0}^{N-1} |\tilde{w}_n|^2 = \sigma_w^2 = \frac{1}{2N} \sum_{n=0}^{N-1} |\tilde{r}_n - \tilde{x}_n|^2. \quad (54)$$

The received signal power over two-dimensions is

$$\begin{aligned}
 \frac{1}{N} \sum_{n=0}^{N-1} |\tilde{r}_n|^2 &= \frac{1}{N} \sum_{n=0}^{N-1} |\tilde{x}_n + \tilde{w}_n|^2 \\
 &= \frac{1}{N} \sum_{n=0}^{N-1} |\tilde{x}_n|^2 + |\tilde{w}_n|^2 \\
 &= P'_{av} + 2\sigma_w'^2 \\
 &= E \left[ |\tilde{x}_n + \tilde{w}_n|^2 \right] \quad (55)
 \end{aligned}$$

where we have assumed independence between  $\tilde{x}_n$  and  $\tilde{w}_n$  and the fact that  $\tilde{w}_n$  has zero-mean. Note that in (55) it is necessary that either  $\tilde{x}_n$  or  $\tilde{w}_n$  or both, have zero-mean.

Next, we observe that (54) is the expression for a  $2N$ -dimensional noise hypersphere with radius  $\sigma_w' \sqrt{2N}$ . Similarly, (55) is the expression for a  $2N$ -dimensional received signal hypersphere with radius  $\sqrt{N(P'_{av} + 2\sigma_w'^2)}$ .

Now, the problem statement is: how many noise hyperspheres (messages) can fit into the received signal hypersphere, such that the noise hyperspheres do not overlap (reliable decoding), for a given  $N$ ,  $P'_{av}$  and  $\sigma_w'^2$ ? The solution lies in the volume of the two hyperspheres. Note that a  $2N$ -dimensional hypersphere of radius  $R$  has a volume proportional to  $R^{2N}$ . Therefore, the number of possible messages is

$$M = \frac{\left( N \left( P'_{av} + 2\sigma_w'^2 \right) \right)^N}{(2N\sigma_w'^2)^N} = \left( \frac{P'_{av} + 2\sigma_w'^2}{2\sigma_w'^2} \right)^N \quad (56)$$

over  $N$  samples (transmissions). The number of bits required to represent each message is  $\log_2(M)$ , over  $N$  transmissions. Therefore, the number of bits per transmission, defined as the channel capacity, is given by [22]

$$\begin{aligned}
 C &= \frac{1}{N} \log_2(M) \\
 &= \log_2 \left( 1 + \frac{P'_{av}}{2\sigma_w'^2} \right) \quad \text{bits per transmission} \quad (57)
 \end{aligned}$$

over two dimensions or one complex dimension (here again the term ‘‘dimension’’ implies a communication link between the transmitter and receiver, carrying only real-valued signals. This is not to be confused with the  $2N$ -dimensional hypersphere mentioned earlier or the  $M$ -dimensional orthogonal constellations in [23]).

*Proposition A.1:* Clearly, the channel capacity is additive over the number of dimensions. In other words, channel capacity over  $D$  dimensions, is equal to the sum of the capacities over each dimension, provided the information is independent across dimensions [11]. Independence of information also implies that, the bits transmitted over one dimension is not the interleaved version of the bits transmitted over any other dimension.

*Proposition A.2:* Conversely, if  $C$  bits per transmission are sent over  $2N_r$  dimensions, ( $N_r$  complex dimensions), it seems reasonable to assume that each complex dimension receives  $C/N_r$  bits per transmission [11].

Note that, when

$$\begin{aligned}
 \tilde{x}_n &= \sum_{n_t=1}^{N_t} \tilde{H}_{k,n,n_r,n_t} S_{k,3,n,n_t} \\
 \tilde{w}_n &= \tilde{W}_{k,n,n_r} \quad (58)
 \end{aligned}$$

as given in (45), the channel capacity remains the same as in (57). We now define the average SNR per bit for MIMO systems having  $N_t$  transmit and  $N_r$  receive antennas. We assume that  $\kappa$  information bits are transmitted simultaneously from each transmit antenna. The amount of information received by each receive antenna is  $\kappa N_t/N_r$  bits per transmission, over two dimensions (due to Proposition A.2). Assuming independent channel frequency response and symbols across different transmit antennas, the average SNR of  $\tilde{R}_{k,i,n_r}$  in (45) can be computed from (46) as:

$$\text{SNR}_{av} = \frac{2L_h\sigma_f^2 P_{av} N_t}{2L_d\sigma_w^2} = \frac{P'_{av}}{2\sigma_w'^2} \quad (59)$$

for  $\kappa N_t/N_r$  bits, where

$$P_{av} = E \left[ |S_{k,3,i,n_t}|^2 \right]. \quad (60)$$

The average SNR per bit is

$$\begin{aligned}
 \text{SNR}_{av,b} &= \frac{2L_h\sigma_f^2 P_{av} N_t}{2L_d\sigma_w^2} \cdot \frac{N_r}{\kappa N_t} \\
 &= \frac{L_h\sigma_f^2 P_{av} N_r}{L_d\sigma_w^2 \kappa} \\
 &= \frac{P'_{av}}{2\sigma_w'^2} \cdot \frac{N_r}{\kappa N_t}. \quad (61)
 \end{aligned}$$

Moreover, for each receive antenna we have

$$C = \kappa N_t/N_r \quad \text{bits per transmission} \quad (62)$$

over two dimensions. Substituting (61) and (62) in (57) we get

$$\begin{aligned}
 C &= \log_2 \left( 1 + C \cdot \text{SNR}_{av,b} \right) \\
 \Rightarrow \text{SNR}_{av,b} &= \frac{2^C - 1}{C}. \quad (63)
 \end{aligned}$$

Clearly as  $C \rightarrow 0$ ,  $\text{SNR}_{av,b} \rightarrow \ln(2)$ , which is the minimum SNR required for error-free transmission over MIMO fading channels.

## REFERENCES

- [1] J. G. Andrews *et al.*, ‘‘What will 5g be?’’ *IEEE Journal on Selected Areas in Communications*, vol. 32, no. 6, pp. 1065–1082, June 2014.
- [2] C. L. I *et al.*, ‘‘New paradigm of 5g wireless internet,’’ *IEEE Journal on Selected Areas in Communications*, vol. 34, no. 3, pp. 474–482, March 2016.
- [3] O. Galinina, A. Pyattaev, S. Andreev, M. Dohler, and Y. Koucheryav, ‘‘5g multi-rat lte-wifi ultra-dense small cells: Performance dynamics, architecture, and trends,’’ *IEEE Journal on Selected Areas in Communications*, vol. 33, no. 6, pp. 1224–1240, June 2015.
- [4] J. Hoydis, S. ten Brink, and M. Debbah, ‘‘Massive mimo in the ul/dl of cellular networks: How many antennas do we need?’’ *IEEE Journal on Selected Areas in Communications*, vol. 31, no. 2, pp. 160–171, February 2013.

- [5] F. Rusek *et al.*, “Scaling up mimo: Opportunities and challenges with very large arrays,” *IEEE Signal Processing Magazine*, vol. 30, no. 1, pp. 40–60, Jan 2013.
- [6] E. Bjrnson, E. G. Larsson, and M. Debbah, “Massive mimo for maximal spectral efficiency: How many users and pilots should be allocated?” *IEEE Transactions on Wireless Communications*, vol. 15, no. 2, pp. 1293–1308, Feb 2016.
- [7] T. S. Rappaport, W. Roh, and K. Cheun, “Mobile’s millimeter-wave makeover,” *IEEE Spectrum*, vol. 51, no. 9, pp. 34–58, Sept 2014.
- [8] Z. Pi and F. Khan, “An introduction to millimeter-wave mobile broadband systems,” *IEEE Communications Magazine*, vol. 49, no. 6, pp. 101–107, June 2011.
- [9] T. S. Rappaport *et al.*, “Millimeter wave mobile communications for 5g cellular: It will work!” *IEEE Access*, vol. 1, pp. 335–349, 2013.
- [10] —, “Broadband millimeter-wave propagation measurements and models using adaptive-beam antennas for outdoor urban cellular communications,” *IEEE Transactions on Antennas and Propagation*, vol. 61, no. 4, pp. 1850–1859, April 2013.
- [11] K. Vasudevan, “Coherent detection of turbo-coded ofdm signals transmitted through frequency selective rayleigh fading channels with receiver diversity and increased throughput,” *Wireless Personal Communications*, vol. 82, no. 3, pp. 1623–1642, 2015. [Online]. Available: <http://dx.doi.org/10.1007/s11277-015-2303-8>
- [12] A. Goldsmith, S. A. Jafar, N. Jindal, and S. Vishwanath, “Capacity limits of mimo channels,” *IEEE Journal on Selected Areas in Communications*, vol. 21, no. 5, pp. 684–702, June 2003.
- [13] Y. Wang and D. W. Yue, “Capacity of mimo rayleigh fading channels in the presence of interference and receive correlation,” *IEEE Transactions on Vehicular Technology*, vol. 58, no. 8, pp. 4398–4405, Oct 2009.
- [14] F. Benkhelifa, A. Tall, Z. Rezki, and M. S. Alouini, “On the low snr capacity of mimo fading channels with imperfect channel state information,” *IEEE Transactions on Communications*, vol. 62, no. 6, pp. 1921–1930, June 2014.
- [15] K. Vasudevan, “Coherent detection of turbo coded ofdm signals transmitted through frequency selective rayleigh fading channels,” in *Signal Processing, Computing and Control (ISPC), 2013 IEEE International Conference on*, Sept 2013, pp. 1–6.
- [16] —, “Coherent detection of turbo-coded OFDM signals transmitted through frequency selective rayleigh fading channels with receiver diversity and increased throughput,” *CoRR*, vol. abs/1511.00776, 2015. [Online]. Available: <http://arxiv.org/abs/1511.00776>
- [17] —, *Digital Communications and Signal Processing, Second edition (CDROM included)*. Universities Press (India), Hyderabad, [www.universitiespress.com](http://www.universitiespress.com), 2010.
- [18] H. Minn, V. K. Bhargava, and K. B. Letaief, “A Robust Timing and Frequency Synchronization for OFDM Systems,” *IEEE Trans. on Wireless Commun.*, vol. 2, no. 4, pp. 822–839, July 2003.
- [19] B. Farhang-Boroujeny, “Ofdm versus filter bank multicarrier,” *IEEE Signal Processing Magazine*, vol. 28, no. 3, pp. 92–112, May 2011.
- [20] S. Haykin, *Adaptive Filter Theory*, 3rd ed. Prentice Hall, 1996.
- [21] K. Vasudevan, “Iterative Detection of Turbo Coded Offset QPSK in the Presence of Frequency and Clock Offsets and AWGN,” *Signal, Image and Video Processing, Springer*, vol. 6, no. 4, pp. 557–567, Nov. 2012.
- [22] J. G. Proakis and M. Salehi, *Fundamentals of Communication Systems*. Pearson Education Inc., 2005.
- [23] K. Vasudevan, “Digital Communications and Signal Processing, Third edition,” 2016, URL: <http://home.iitk.ac.in/vasu/book0.pdf> [accessed: 2016-09-26].